Supplementary Material

DNA Damage Recognition and Repair by 3-Methyladenine DNA Glycosylase I (TAG)

Audrey H. Metz, Thomas Hollis, and Brandt F. Eichman

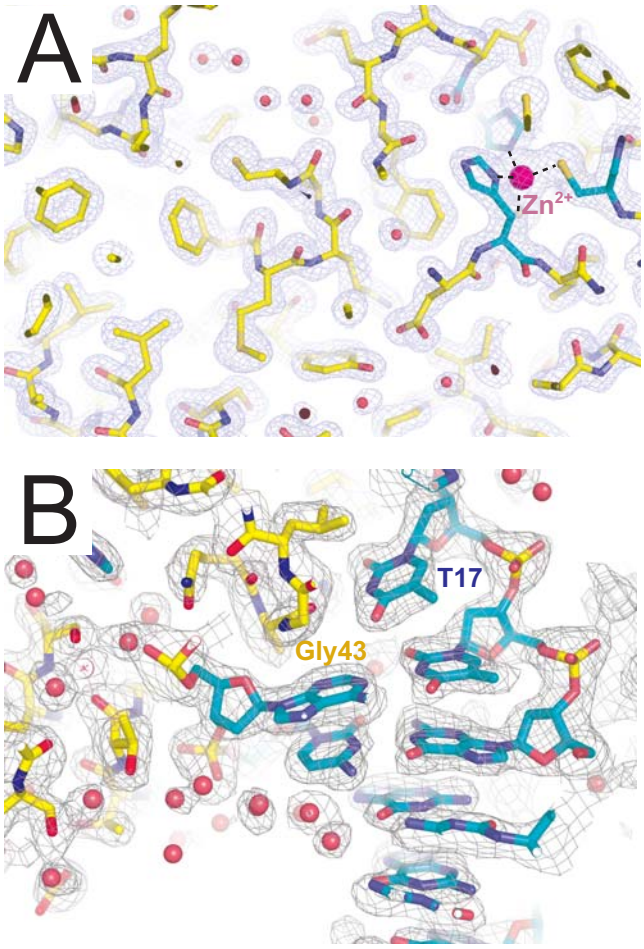

Figure S1. Experimental electron density for TAG (A) and TAG-DNA (B). (A) A cross section of the final refined TAG model superimposed on the 1.5 Å solvent-flattened Se-MAD electron density map contoured at 1σ. Side chains coordinating Zn^{2+} (magenta sphere) are colored blue. (B) Cross section of the TAG-DNA structure and solvent-flattened Se-SAD electron density contoured at 1σ. DNA carbon atoms are colored blue. The Gly43 plug and estranged thymine T17 are labeled for reference.

A

```
Ec TAG    MERCGWVSQDPLYIAYHDNEWGVPETDSKKLFEMICLEGQQAGLSWITVLKKRENYRACF 60
St TAG    MQRCDWVSQDPLYIAYHDNEWGVPETDSRKLFEMICLEGQQAGLSWITVLKKRENYRACF 60

Ec TAG    HQFDPVKVAAMQEEDVERLVQDAGIIRHRGKIQAIIGNARAYLQMEQNGEPFVDFVWSFV 120
St TAG    HQFDPIRIAAMQEEDVERLLQNTGIIRHRGKIQAIISNARAWLAMEQNGESFADFVWSFV 120

Ec TAG    NHQPQVTQATTLSEIPTSTSASDALSKALKKRGFKFVGTTICYSFMQACGLVNDHVVGCC 180
St TAG    DGQPQITQAASLDKIPTSTPASDALAKALKKRGFKFVGTTICYSFMQACGLVNDHITGCF 180

Ec TAG    CYPGNKP------ 187
St TAG    CHPGEKHDSQIPE 193
```

B

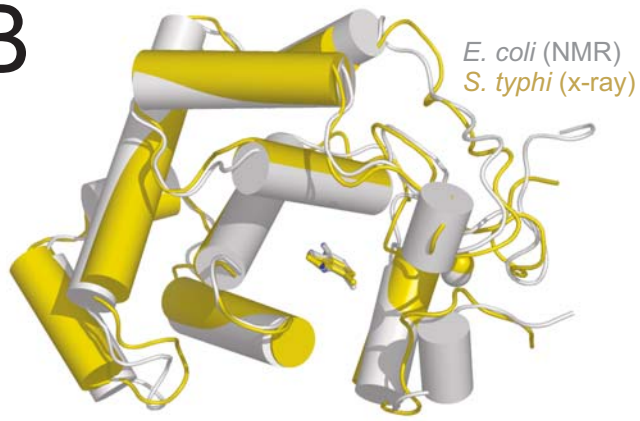

C

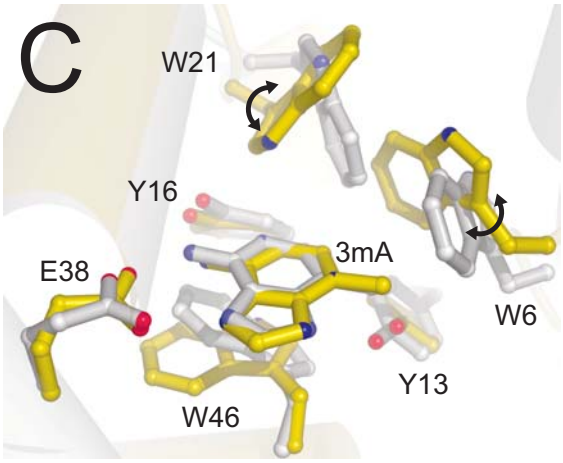

Figure S2. Comparison of *E. coli* and *S. typhi* TAG. (A) Sequence alignment shows identical (red) and conserved (blue) residues. Residues in the active site (gray), contacting the DNA (green), and coordinating Zn^{2+} (yellow) are identical between the two proteins. Residues shown to affect 3mA binding (*E. coli*) or catalysis (*S. typhi*) are in boldface. (B) Superposition of *E. coli* (NMR, 1P7M, silver) and *S. typhi* (X-ray, this work, gold) TAG/3mA structures. Bound 3mA base is shown as ball-and-sticks in the center of the figure. (C) Details of the active sites of the NMR (silver) and crystal (gold) structures show deviations in side chain rotamers for Trp21 and Trp6.

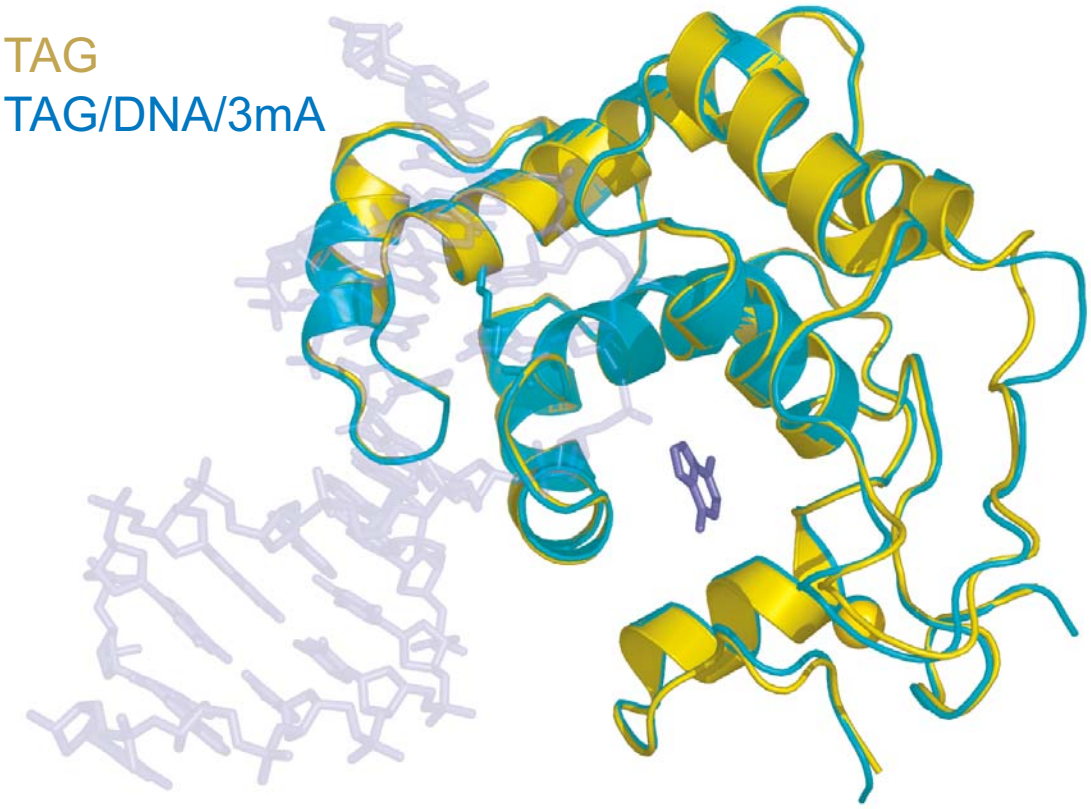

Figure S3. Comparison of TAG in the presence and absence of DNA. Ribbon representation of crystal structures of *S. typhi* TAG in the free (gold) and DNA-bound (blue) state shows no significant differences between the two models. The bound DNA and 3mA base are shown as blue sticks.

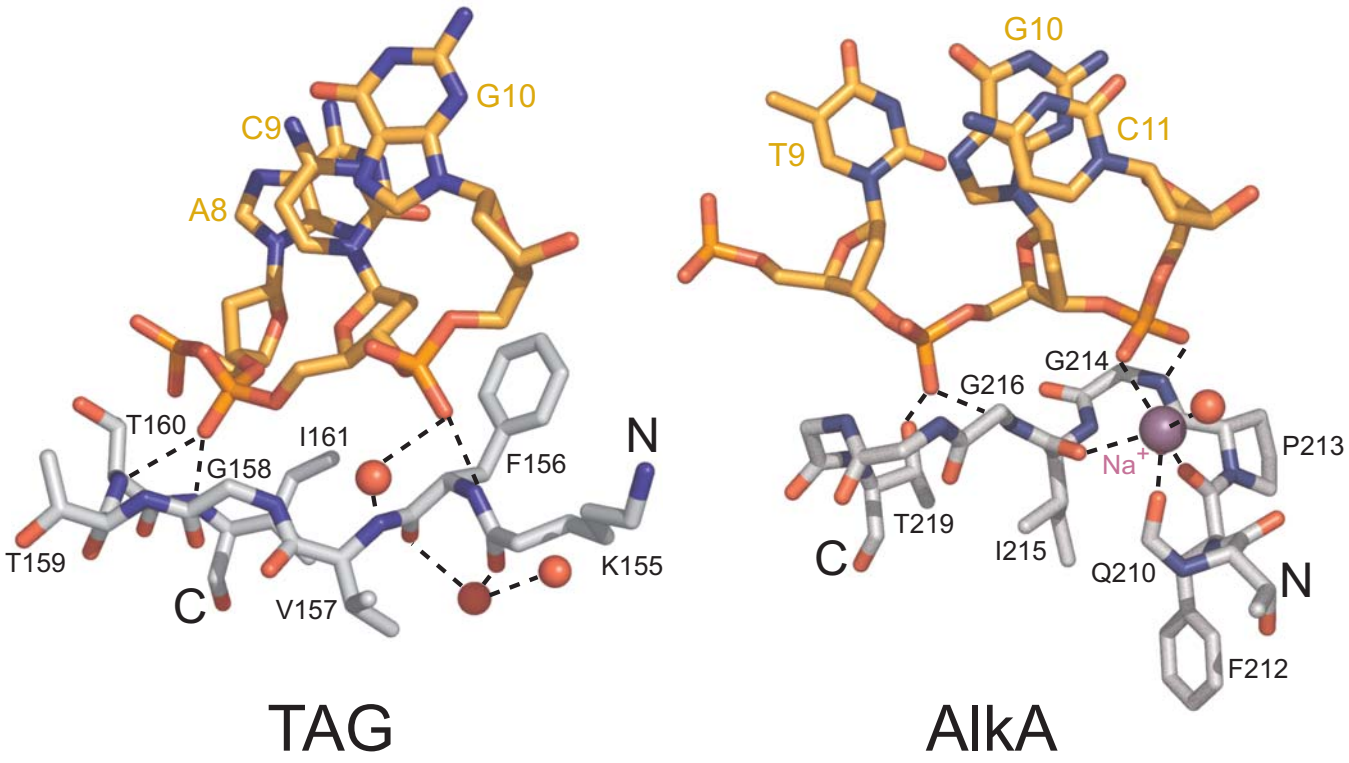

Figure S4. The HhH motif of TAG and AlkA. *Left*: The TAG HhH motif anchors the protein to the DNA immediately 3´ to the lesion. TAG contacts the DNA backbone directly through hydrogen bonds with the main chain amides of Gly158, Thr160, Ile161, and Phe156 and indirectly through a water mediated hydrogen bond with the main chain amide of Val157. The hairpin turn does not ligate a cation like other HhH glycosylases, but instead creates a hydrogen bonded network with the main chain carbonyl oxygens of Lys155 and Phe156 and two water molecules (red spheres). *Right*: The AlkA HhH motif also anchors the protein to the damaged DNA strand. AlkA directly contacts the DNA backbone through hydrogen bonds with Thr219 and the main chain amides of Gly216 and Gly214. The hairpin turn is presumably stabilized by a sodium ion (purple sphere) that is coordinated by Ile215, Phe212, and Gln210 main chain carbonyl oxygens, a DNA phosphate oxygen, and a water molecule (red sphere).

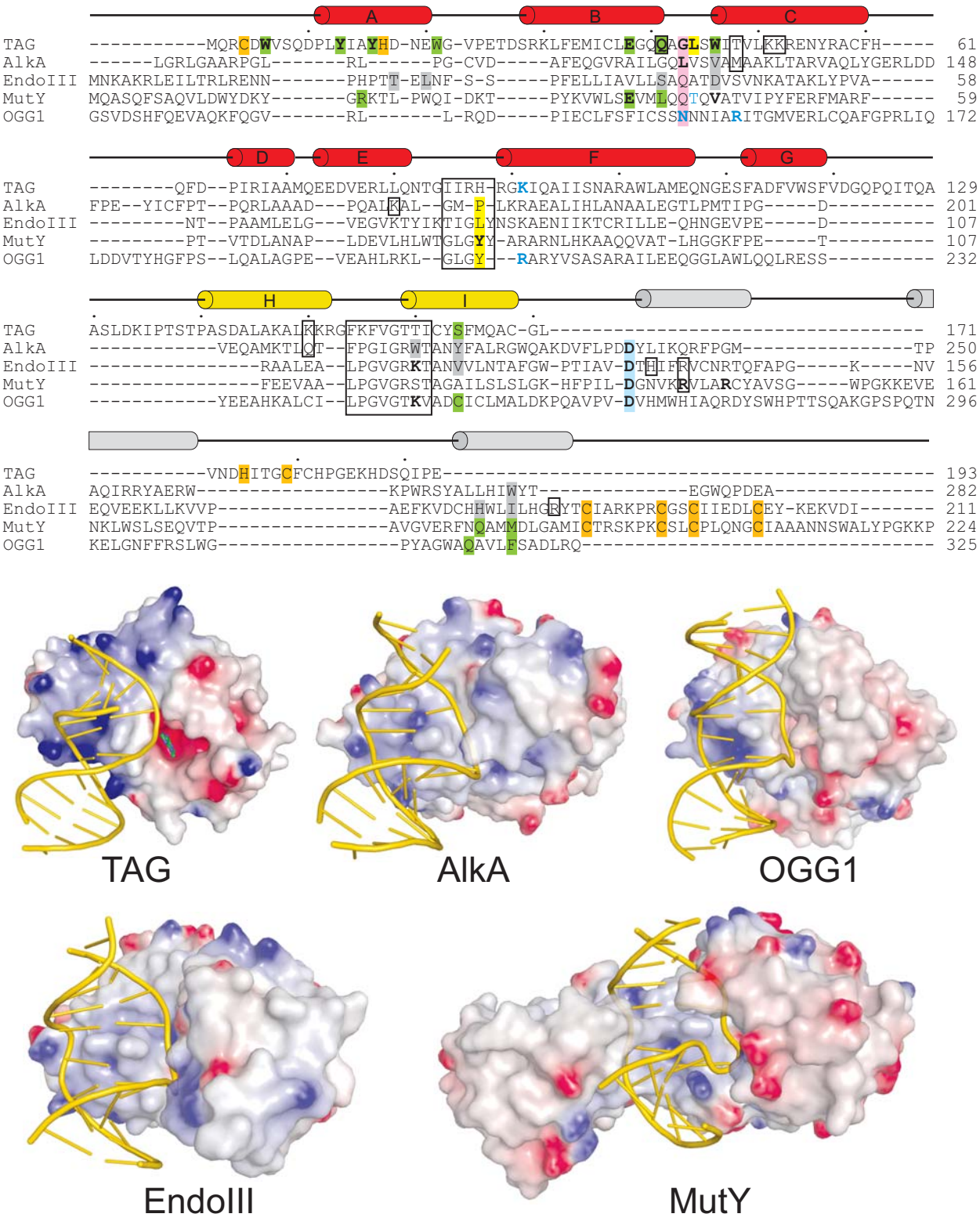

Figure S5. The HhH superfamily of DNA glycosylases. *Top*: Structure-based sequence alignment shows the relative position of residues important for DNA binding and base excision. Secondary structure elements are shown schematically, with the HhH motif in yellow and helices not present in TAG in grey. Residues contacting the DNA backbone are boxed, intercalating plug (yellow) and wedge (pink) residues are shaded, and side chains contacting the estranged base are labeled blue. Active site side chains confirmed/postulated to contact the substrate base are shaded green/grey, and the conserved catalytic aspartate is shaded blue. Residues verified biochemically to affect substrate binding or catalysis are shown in boldface. Zn^{2+}-binding residues (TAG) and Fe_4Se_4 cluster cysteines (MutY, EndoIII) are shaded orange. *Bottom*: Crystal structures of HhH glycosylase/DNA complexes are shown as electrostatic surfaces (red, negative; blue positive). TAG, 2OFI (this work); AlkA, 1DIZ; hOgg1, 1EBM ; EndoIII, 1P59 ; MutY, 1RRQ .

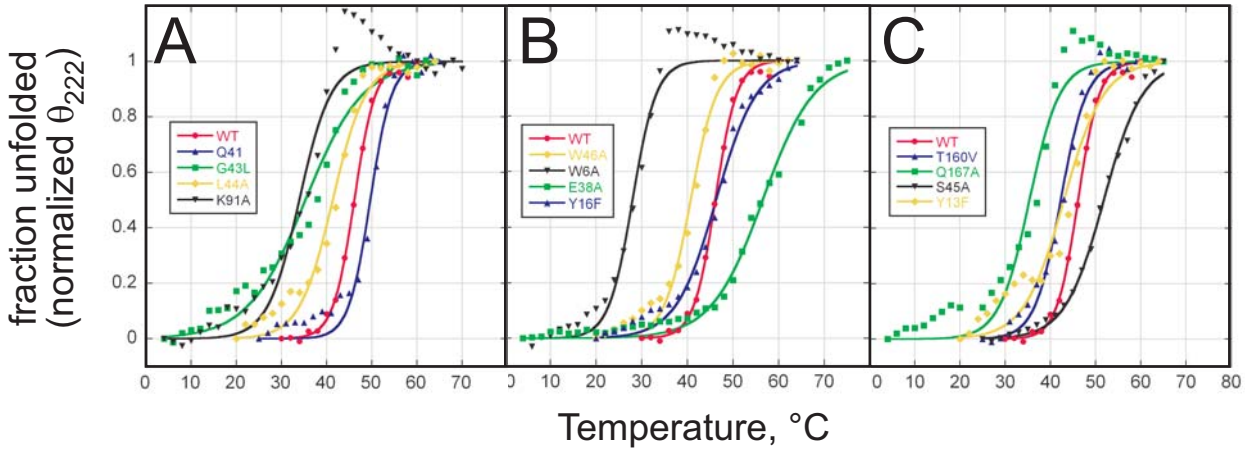

mutant	T_m (ºC)
WT	46.1
L44A	41.3
G43L	35.3
K91A	34.0
Q41A	49.7
E38A	56.5
Y16F	46.3
W46A	40.7
W6A	27.7
Y13F	43.0
T160V	42.3
S45A	51.8
Q167A	37.8

Figure S6. Thermal denaturation of TAG mutants. Protein unfolding was monitored by circular dichroism spectroscopy and following the change in molar elipticity at 222 nm as a function of temperature. Melting curves are grouped according to residue locale: (A) residues intercalating the DNA abasic site, (B) active site residues, and (C) other residues in the 3mA binding pocket. Melting temperatures (T_m) shown in the table were derived from fits to the CD data using the equation $\theta = 1/(1+e^{(T_m-T)/k})$, where T_m corresponds to the temperature at 50% denaturation, and *k* describes the cooperativity of the transition.

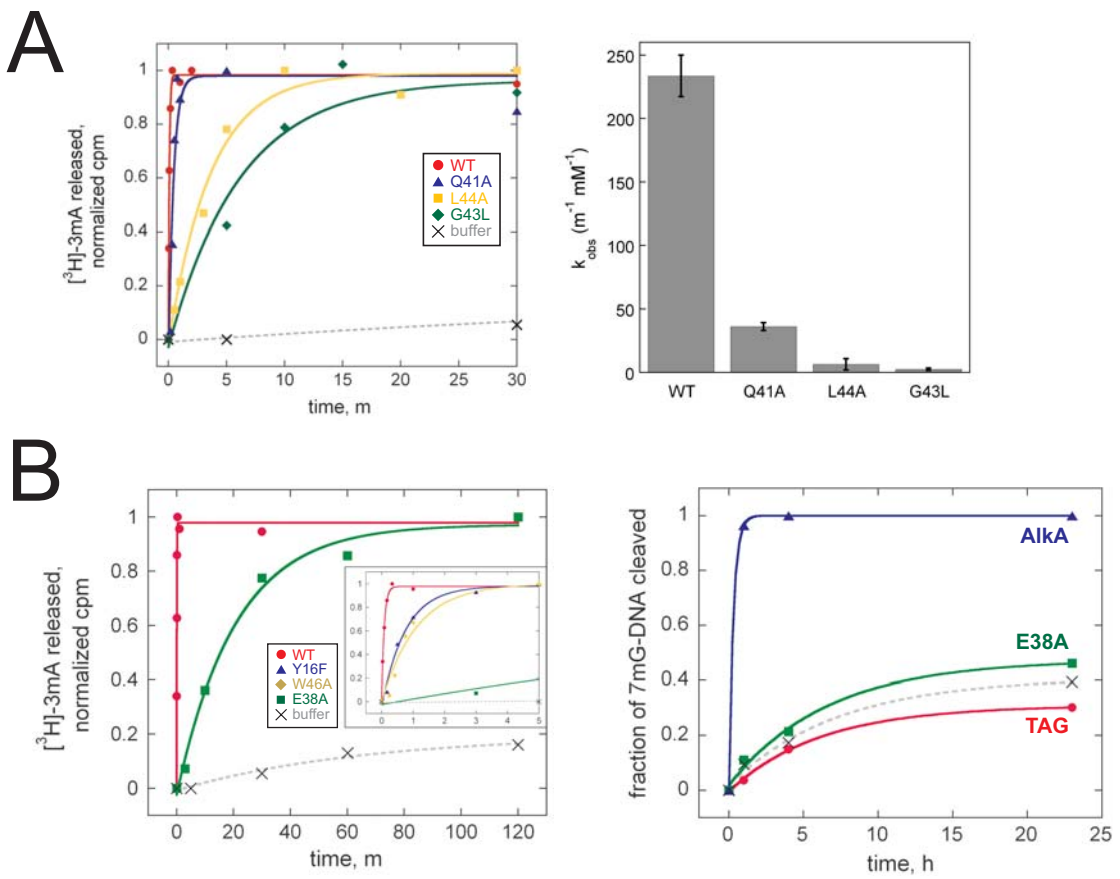

Figure S7. Base excision activity of TAG intercalating (A) and active site (B) mutants. (A) Kinetic traces (left) show the decrease in rates of 3mA excision from genomic DNA by intercalating mutants as compared to wild-type TAG. Extracted average rate constants for each mutant are compared in the bar graph to the right. Error bars represent the standard deviation from three experiments. (B) Time course for excision of 3mA from genomic DNA by TAG active site mutants are shown to the left. The inset shows the effects of Y16F (blue triangles) and W46A (yellow diamond) mutants as compared to wild-type (red circles) and E38A (green squares) in the first 5 min of the reaction. The graph on the right shows the inability of wild-type and E38A TAG to excise 7mG from a defined oligonucleotide substrate. AlkA excision of 7mG from this substrate is shown as a positive control (blue triangles). 7mG glycosylase activity was measured by alkaline cleavage of the abasic-DNA product of base excision from a 25mer oligonucleotide duplex containing a 7mG·C base pair. 7mG was incorporated enzymatically using the appropriate primer/template and DNA polymerase I Klenow fragment (New England Biolabs) . In a 10 µl reaction, 2 nM radiolabeled DNA duplex was incubated with 3 µM enzyme in activity buffer. The reaction was quenched at various times by addition of 0.2 N NaOH, and heated at 70° C for 10 min. Products and remaining substrate were separated by denaturing polyacrylamide gel electrophoresis and quantitated by autoradiography. Under the conditions of this assay, the enzyme concentration is saturating with respect to substrate.

References

Asaeda, A., Ide, H., Asagoshi, K., Matsuyama, S., Tano, K., Murakami, A., Takamori, Y. and Kubo, K. (2000) Substrate specificity of human methylpurine DNA *N*-glycosylase. *Biochemistry*, **39**, 1959-1965.

Bruner, S.D., Norman, D.P. and Verdine, G.L. (2000) Structural basis for recognition and repair of the endogenous mutagen 8-oxoguanine in DNA. *Nature*, **403**, 859-866.

Fromme, J.C., Banerjee, A., Huang, S.J. and Verdine, G.L. (2004) Structural basis for removal of adenine mispaired with 8-oxoguanine by MutY adenine DNA glycosylase. *Nature*, **427**, 652-656.

Fromme, J.C. and Verdine, G.L. (2003) Structure of a trapped endonuclease III-DNA covalent intermediate. *Embo J*, **22**, 3461-3471.

Hollis, T., Ichikawa, Y. and Ellenberger, T. (2000) DNA bending and a flip-out mechanism for base excision by the helix-hairpin-helix DNA glycosylase, *Escherichia coli* AlkA. *Embo J*, **19**, 758-766.